

Energy loss mechanism for suspended micro- and nanoresonators due to the Casimir force

André Gusso*

Departamento de Ciências Exatas-EEIMVR, Universidade Federal Fluminense, Volta Redonda 27255-125, RJ, Brazil

(Received 5 July 2009; revised manuscript received 14 December 2009; published 26 January 2010)

A so far not considered energy loss mechanism in suspended micro- and nanoresonators due to noncontact acoustical energy loss is investigated theoretically. The mechanism consists on the conversion of the mechanical energy from the vibratory motion of the resonator into acoustic waves on large nearby structures, such as the substrate, due to the coupling between the resonator and those structures resulting from the Casimir force acting over the separation gaps. Analytical expressions for the resulting quality factor Q for cantilever and bridge micro- and nanoresonators in close proximity to an underlying substrate are derived and the relevance of the mechanism is investigated, demonstrating its importance when nanometric gaps are involved.

DOI: [10.1103/PhysRevB.81.035425](https://doi.org/10.1103/PhysRevB.81.035425)

PACS number(s): 62.25.-g, 62.30.+d, 85.85.+j

I. INTRODUCTION

High quality factor suspended micro- and nanoresonators are required in order to make practical several potential applications of such mechanical resonators as replacements for electronic filters and reference frequency resonators as well as ultrasensitive mass, force, charge, spin, and chemical sensors.^{1,2} For microresonators (characterized by having at least two dimensions in the micrometer range) the Q values usually range from $\mathcal{O}(10^4)$ up to $\mathcal{O}(10^5)$. For nanoresonators (having at least two dimensions in the submicrometer range) it has usually been the case that Q hardly exceeds 10^4 (Ref. 3), however, more recently, nanomechanical beam resonators set to vibrate as nanostrings resulted to have $Q \sim 4 \times 10^5$ (Ref. 4), and nanoresonators based on GaN nanowires vibrating in the megahertz range were reported to achieve $Q=4 \times 10^6$ (Ref. 5). As new designs and fabrication processes are created in order to overcome the known energy loss mechanisms,⁶ specially clamping loss and surface defects, very high Q micro- and nanoresonators can be expected to be available for practical applications. However, as known energy loss mechanisms are overcome increasing the quality factor, new mechanisms previously ignored can start to set new limits on Q .

In this work a so far not considered energy loss mechanism is investigated. This investigation is motivated by the fact that in most practical applications the resonators are expected to have their motion driven and detected electrostatically, that means capacitively, in designs involving very small gaps extending over large areas between the resonator and the electrodes. For instance, in the current practical designs of rf microelectromechanical systems (MEMS) filters, sub-100 nm gaps are usually required for adequate electromechanical coupling² and while gaps as small as 20 nm where already employed⁷ even smaller gaps were envisaged as necessary for MEMS filters operation using complementary metal-oxide-semiconductor (CMOS) drive voltage.⁸ Besides, gaps in the nanometer range are a natural consequence of the miniaturization toward nanoelectromechanical systems (NEMS) filters and other devices.

The energy loss mechanism analyzed in this work results from the coupling between the resonator and the nearby structures established across vacuum or air gaps by an attrac-

tive Casimir force. For instance, in micro- and nanoelectromechanical resonators the nearby structures could correspond to large area electrodes built on top of the substrate and located beneath the resonator, as is usually the case for beam resonators, or the electrodes surrounding a disk resonator.² Due to the coupling across the gap the motion of the resonator results in a time-varying force on the surface of the nearby structures. This force induces the surface to oscillate at the same frequency resulting in acoustic emissions that carry away a fraction of the resonator mechanical energy. Such noncontact acoustical energy loss was considered previously in the context of tip-sample interaction in atomic force microscopy⁹ due to the van der Waals force between metals and is generalized here to the interaction between the surface of micro- and nanoresonators with its surroundings mediated by the Casimir force, calculated using the full Lifshitz theory. In the present work this mechanism is analyzed in details for the case of suspended beam resonators, considered to be located on top of a substrate. Because in practice the substrate is much larger than the micro- and nanoresonators we consider in this analysis it is modeled as a semispace. As simplifying assumptions both the beam and the substrate are assumed to be made from a homogeneous isotropic material, and their motion is considered adiabatic (purely elastic).

II. ENERGY LOSS MECHANISM**A. Casimir force**

The Casimir force, which gives rise to the new energy loss mechanism, has the same physical origin as the van der Waals force, resulting from the quantum fluctuations of the vacuum electromagnetic field.¹⁰ However, while in a simplified picture the van der Waals force can be understood as resulting from the propagation of virtual nonretarded electromagnetic waves, resulting in a short range effect, the Casimir force originates from the retarded waves that act at larger distances, extending the range of action of the quantum fluctuations. Because the Casimir force becomes relevant in the submicrometer range, its impact on the operation of MEMS and NEMS has been receiving increasing attention.^{11,12} In general, this peculiar force depends on the geometry and the

optical properties of the boundaries, however, our analysis requires solely the knowledge of the negative (attractive) pressure between two semispaces as first derived by Lifshitz.¹³ The final expression for the force is a function of the optical properties of the semispaces through the frequency dependent complex dielectric function. Using the Lifshitz theory the Casimir force between semispaces made from materials relevant for the fabrication of micro- and nanoresonators was calculated in Ref. 14. Following this last work and the references therein, we express the Casimir force for real boundaries in terms of a correction factor to the pressure predicted for two perfectly conducting plates $P^0(d) = -\pi^2 \hbar c / (240d^4)$, namely,

$$P(d) = -\eta(d) \frac{\pi^2 \hbar c}{240 d^4} = -\eta(d) \frac{C}{d^4} = \eta(d) P^0(d), \quad (1)$$

where d denotes the gap between the surfaces, \hbar the Planck constant over 2π , c is the speed of light, and the constant C incorporates the constant factors in the above expression for later convenience. The factor $\eta(d)$ is usually referred to as the finite conductivity correction factor, derived from the actual dielectric properties of the surfaces involved using the Lifshitz theory. For all known materials $\eta(d) < 1$, therefore, the pressure between two parallel surfaces made from actual materials is always smaller than the pressure between perfectly conducting plates P^0 . The analysis presented in Ref. 14 indicates the relevance of this correction factor, which is as small as 0.088 for silicon surfaces separated by a 10 nm gap, and cannot be simply ignored.

B. Acoustic emission and the quality factor

Here we consider the setup were a rectangular cantilever or bridge resonator of length l , width w and height h is placed a distance d above the substrate. When the resonator is set to vibrate in a given mode with time-varying vertical displacement $u_n(x, t) = u_n(x) \exp(i\omega_n t)$ the gap varies according to $d - u_n(x, t)$ resulting, in the small displacement approximation, in a time-varying Casimir force on the substrate. For an infinitesimal rectangular element with length dx this force is

$$dF(x, t) = C \frac{\eta(d - u_n(x, t))}{[d - u_n(x, t)]^4} w dx \approx C \frac{\eta(d)}{d^4} w dx + 4C \frac{\eta(d)}{d^5} w u_n(x) e^{i\omega_n t} dx. \quad (2)$$

The first term represents a constant force and can be ignored. It is the second time-varying term proportional to $u_n(x)$ which induces a time-varying displacement of substrate surface that, in its turn, results on the emission of acoustic waves with frequency ω_n . The wavelength λ of the waves produced on the substrate can be shown to be related to the dimensions of the resonator by the approximate relation $\lambda \sim (l/h)l$, valid for the frequencies generated by the first three modes. Because for most practical devices $l/h \geq 10$ and $w < l$, λ is large compared with the lateral dimensions of the source, therefore, justifying the use of the point source approximation. In this approximation the details on the force

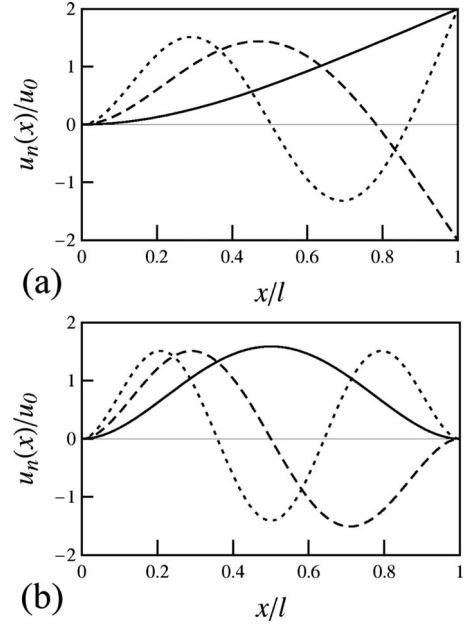


FIG. 1. Mode shapes for the three lowest frequencies $n=1$ (continuous), 2 (dashed), and 3 (dotted) for (a) cantilever and (b) bridge resonators.

distribution over the source are not of fundamental importance for the calculation of the irradiated acoustic power. However, some aspects of the force distribution must be taken into account as we do next.

First, we note that in most practical applications of beam micro- and nanoresonators the ratio h/l is sufficiently small to the Euler-Bernoulli beam theory to apply,¹⁵ at least approximately. In this case the resulting mode shapes are given by a general expression of the form

$$u_n(x) = u_0 \{ \cosh(\kappa_n x/l) - \cos(\kappa_n x/l) + \chi_n [\sinh(\kappa_n x/l) - \sin(\kappa_n x/l)] \}, \quad (3)$$

where for the first three modes of the cantilever (bridge) we have $\kappa_1 = 1.8751(4.7300)$, $\kappa_2 = 4.6941(7.8532)$, $\kappa_3 = 7.8548(10.996)$, and $\chi_1 = -0.7341(-0.9825)$, $\chi_2 = -1.0185(-1.0008)$, and $\chi_3 = -0.9992(-0.9999)$. In Fig. 1, $u_n(x)$ for the first three modes of cantilever and bridge are presented. As seen from the second term in Eq. (2) the amplitude of the time-varying force on the surface varies in position following $u_n(x)$. Therefore, all the points of the source region on the surface are in phase for the first mode of both the cantilever and bridge, and both sources can be held as acoustic monopoles. For the second mode of the bridge, points to the left and to the right of the midpoint vibrate out of phase by 180° and the source can be treated as an acoustic dipole. Before discussing how the acoustic emissions produced by the other vibrating modes can be held, let us consider the acoustic emission by the monopoles and dipoles on the surface.

Miller and Pursey¹⁶ were the first to derive from the elasticity theory an expression for the acoustic energy emitted by a point source vibrating normal to the surface of a semispace.

For an harmonically varying force of the form $F(t) = F \exp(i\omega_n t)$ they employed the admittance method obtaining¹⁶

$$\Pi^m = \frac{1}{4\pi} \frac{\sqrt{\rho^s C_{11}^s}}{C_{44}^s} \omega_n^2 F^2 \phi_m(\gamma), \quad (4)$$

where $\phi_m(\gamma)$ corresponds to

$$\phi_m(\gamma) = \text{Im} \left[\int_0^\infty \frac{p\sqrt{p^2-1}}{F_0(p, \gamma)} dp \right], \quad (5)$$

with

$$F_0(p, \gamma) = (2p^2 - \gamma^2)^2 - 4p^2 \sqrt{p^2-1} \sqrt{p^2-\gamma^2}, \quad (6)$$

and $\gamma = \sqrt{C_{11}^s/C_{44}^s}$, ρ^s is the density, C_{11}^s and C_{44}^s are the elastic stiffness coefficients that characterize the isotropic material of the substrate, as indicated by the superscript s . Several authors have rederived Eq. (4) since the now classical work of Miller and Pursey, however, differing in the definition¹⁷ or on the evaluation^{9,18} of $\phi_m(\gamma)$. In the original work¹⁶ the integral was evaluated numerically taking into account the branch-points $p=1$, γ , the principal value of the radicals, and the only physically relevant pole satisfying the condition $p > \gamma$. Following the prescriptions given by Miller and Pursey in the Sec. 7 of Ref. 16 we derive another representation suitable for numerical evaluation

$$\begin{aligned} \phi_m(\gamma) = & \int_0^1 \frac{p\sqrt{1-p^2}}{(2p^2 - \gamma^2)^2 + 4p^2\sqrt{1-p^2}\sqrt{\gamma^2-p^2}} dp \\ & + \int_1^\gamma \frac{4p^3(p^2-1)\sqrt{\gamma^2-p^2}}{(2p^2 - \gamma^2)^4 + 16p^4(p^2-1)(\gamma^2-p^2)} dp \\ & - \pi \frac{p_r \sqrt{p_r^2-1}}{F_0'(p_r, \gamma)}, \end{aligned} \quad (7)$$

where the last term corresponds to the contribution from a clockwise indentation around the pole at $p=p_r$, determined as the root of $F_0(p, \gamma)=0$ satisfying $p_r > \gamma$. The above representation was checked to reproduce the numerical result reported by Miller and Pursey for $\gamma=\sqrt{3}$, $\phi_m(\sqrt{3})=0.537$, and to differ only slightly from the result reported by Hunter¹⁹ for $\gamma=2$, $\phi_m(2)=0.415$, in which case we obtain $\phi_m(2)=0.409$, a difference that may be due to numerical precision. It is worth to note that in Ref. 17, in spite of the fact that the authors base their analysis on the work of Miller and Pursey, the expression for the acoustic power Π^m contains an integral that, while similar to that in Eq. (5), leads to significant discrepancies in the numerical results, underestimating the emitted acoustic power by as much as a factor of 10. In a recent analysis of the support (or clamping) loss in micromechanical resonators,¹⁸ which also follows the work of Miller and Pursey, exactly the same expression for Π^m given in Eq. (4) was reported. However, the numerical evaluation of $\phi_m(\gamma)$ did not take into account the contribution from the pole at p_r , also leading to a significant underestimate of acoustic emissions. The neglecting of the contribution from the pole corresponds, physically, to neglecting the contribution of the Rayleigh surface waves which are responsible for

carrying away the major fraction of the acoustic energy.¹⁶ In Ref. 9 the acoustic emission by an harmonically varying normal force applied to the surface of a semispace was reconsidered. This work provides a coefficient of friction $\Gamma_\perp = \xi_\perp F^2 / (4\pi\rho^s c_t^3)$, where $c_t = \sqrt{C_{44}^s/\rho^s}$ is the transverse sound velocity, and ξ_\perp corresponds to the sum of three terms similar to those in Eq. (7). From Γ_\perp we can derive the emitted acoustic power defined as,⁹ $\Pi = \Gamma_\perp 2\omega^2 u_0^2$ were, in the notation of Ref. 9, u_0 denotes half the amplitude of the vertical motion which was given as the sum of a complex amplitude proportional to u_0 plus its conjugate. The resulting expression for Π^m is identical to that in Eq. (4) with $\phi_m(\gamma)$ replaced by $\xi_\perp / (2\gamma)$. By means of an adequate change of variables, $\phi_m(\gamma)$ can be made equal to $\xi_\perp / (2\gamma)$, except for the limits of integration of the two integrals in Eq. (7). Therefore, the emitted acoustic power calculated using the expressions provided in Ref. 9 does not match Π^m determined by Miller and Pursey. However, the results can be made to coincide if the limits defined in the two integrals in ξ_\perp are taken squared, in which case they become the same as the limits in Eq. (7) after the proper change of variables, indicating that ξ_\perp should be corrected in this manner.

Specializing to the case of a suspended resonator vibrating transversally in the mode $u_n(x)$, the time-varying contribution from the total applied force on the surface is

$$F(t) = F \exp(i\omega_n t) = 4C\eta(d)d^{-5}w \int_0^l u_n(x) dx \exp(i\omega_n t), \quad (8)$$

Therefore, the energy lost per cycle is $\Delta U_n = \Pi / f_n = 2\pi\Pi / \omega_n$. The resulting quality factor Q is a measure of the ratio of the vibrational energy of the resonator U_n to the energy lost, namely, $Q = 2\pi U_n / \Delta U_n = \omega_n U_n / \Pi$. The vibrational energy for both cantilevers and bridges is $U_n = hwl\rho^r \omega_n^2 u_0^2 / 2$ while the mode frequency is $\omega_n^2 = \kappa_n^4 E^r h^2 / (12\rho^r l^4)$, implying that for the modes considered as acoustic monopoles

$$Q^m = \frac{\pi}{16\sqrt{3}} \frac{\kappa_n^2}{I_{u_n}^2} \frac{1}{C^2 \phi_m(\gamma)} C_{44}^s \left(\frac{E^r \rho^r}{C_{11}^s \rho^s} \right)^{1/2} \frac{h^2}{wl^3} \frac{d^{10}}{\eta(d)^2}, \quad (9)$$

where $I_{u_n} = \int_0^l u_n(x) dx / (u_0 l)$, E^r denotes the Young modulus, and ρ^r the density of the resonator as indicated by the superscript r . The result expressed in Eq. (9) reveals that Q^m is a fast varying function of the gap distance showing an explicit dependence that goes as d^{10} . However, in order to determine the actual dependence of Q^m on d we have to take into account the term $\eta(d)$. From the results presented in Ref. 14 it is generally the case for conductors and semiconductors that $\eta(d) \propto d^\alpha$ with α increasing almost linearly from approximately 0.65 for d equal to 15 nm to values close to 1 at 1 nm. Therefore, in this particular range of distances, Q^m has an exponent for d varying from 8 up to a maximum of approximately 8.7. The dependence on the geometrical parameters h , w , and l indicates that the new energy loss mechanism is more relevant for thin, wide, and long structures. It can also be inferred that Q^m is smaller for soft materials in the substrate due to the dependence on C_{44}^s .

We turn now to the analysis of a dipolar excitation at the surface of the substrate. In this case there is no net vertical force, instead there is a net bending moment M which, due to the symmetry of the second mode for the bridge, results to be

$$M = 8C \frac{\eta(d)}{d^5} w \int_0^{l/2} u_2(x) \left(\frac{l}{2} - x \right) dx. \quad (10)$$

This bending moment causes the surface to twist. For small sources, we can use the average twisting angle calculated by Bycroft²⁰ for an harmonically varying bending moment $M(t) = M \exp(i\omega_n t)$ distributed over a circular region, Eq. (191) of Ref. 20. In the limit of small radius over wavelength ratio the amplitude of the angle is

$$\theta = \frac{Mk^3}{4\pi\gamma C_{44}^s} \phi'_d(\gamma), \quad (11)$$

where

$$\phi'_d(\gamma) = \int_0^\infty \frac{p^3 \sqrt{p^2 - 1}}{F_0(p, \gamma)} dp, \quad (12)$$

and $k = 2\pi/\lambda^s = \omega_n \sqrt{\rho^s/C_{44}^s}$. We implicitly incorporate into the integral the explicit contribution of the physically allowed pole at p_r introduced by Bycroft. This last author also introduces the same explicit contribution into the expression for the average vertical displacement due to an harmonically varying normal force when compared to the result obtained by Miller and Pursey.¹⁶ With this definition for the integral we can proceed to obtain a representation suitable for numerical evaluation following the same procedure adopted for $\phi_m(\gamma)$. As we argue next, in order to determine the emitted acoustic power only the evaluation of the imaginary part of $\phi'_d(\gamma)$ is required, which can be written as

$$\begin{aligned} \phi_d(\gamma) = \text{Im}[\phi'_d(\gamma)] &= \int_0^1 \frac{p^3 \sqrt{1-p^2}}{(2p^2 - \gamma^2)^2 + 4p^2 \sqrt{1-p^2} \sqrt{\gamma^2 - p^2}} dp \\ &+ \int_1^\gamma \frac{4p^5 (p^2 - 1) \sqrt{\gamma^2 - p^2}}{(2p^2 - \gamma^2)^4 + 16p^4 (p^2 - 1) (\gamma^2 - p^2)} dp \\ &- \pi \frac{p_r^3 \sqrt{p_r^2 - 1}}{F'_0(p_r, \gamma)}. \end{aligned} \quad (13)$$

In the complex notation the real and imaginary components of the displacement correspond to the in-phase and out-of-phase components relative to the applied force or moment. Only the out-of-phase component of θ contributes to the time averaged acoustic power through $\Pi = \langle \text{Re}[M(t)] \text{Re}[\dot{\theta}(t)] \rangle = \text{Re}[M \times \dot{\theta}]/2$, where $\langle \rangle$ denotes the time average, M the real amplitude from $M(t)$, and $\dot{\theta} = i\omega_n \theta$ the complex amplitude of the angular velocity. We note that we could have used the analogous definition for the average emitted acoustic power for the normal point source obtaining the same result as in Eq. (4). In this case $\Pi = \langle \text{Re}[F(t)] \text{Re}[\dot{z}(t)] \rangle$, where $z(t) = z \exp(i\omega_n t)$, and z denotes the complex average vertical displacement given by Eq. (129) of Ref. 16. In the case of the dipolar source the resulting emitted power is

$$\Pi^d = \frac{1}{8\pi C_{44}^{s2}} \left(\frac{\rho^s}{C_{11}^s} \right)^{1/2} \omega_n^4 M^2 \phi_d(\gamma). \quad (14)$$

As for Π^m it is worth to compare this result for Π^d with those found in the literature. Compared to the results presented in Ref. 17, also based upon the work of Bycroft, the same difference is found concerning the definition of the denominator in the integral $\phi'(d)$. Our result can also be compared with a derivation for the acoustic energy loss due to an AFM tip vibrating parallel to the surface of a plane substrate.⁹ This is an analogous situation because the harmonic horizontal displacement of the force can be interpreted as resulting into a time-varying harmonic torque about an horizontal axis perpendicular to the direction of the tip vibration. Considering the definition of the horizontal displacement given in Ref. 9, which has amplitude $2u_0$, a point force displacing horizontally results in a torque $M(t) = 2u_0 F \cos(\omega_n t) = M \cos(\omega_n t)$. From the given expression for the friction coefficient (see the Appendix B of Ref. 9)

$$\Gamma_{\parallel} = \frac{\xi_{\parallel}}{8\pi \rho c_t^5} \omega_n^2 F^2, \quad (15)$$

the emitted power $\Pi = \Gamma_{\parallel} 2\omega^2 u_0^2$ results to be the same as that in Eq. (14) with $\phi_d(\gamma)$ replaced by $(\gamma/2)\xi_{\parallel}$, where ξ_{\parallel} is an expression similar to Eq. (13). As for the monopole case, $\phi_d(\gamma)$ can be made to coincide with $(\gamma/2)\xi_{\parallel}$ after an adequate change of variables except for the limits of integration. The two results for Π^d can be made identical if the limits of integration in ξ_{\parallel} are taken squared.

From Eq. (14) we can follow the same procedure as for the monopole in order to calculate the quality factor for the second mode of the bridge which results to be

$$Q^d = \frac{1.222}{C^2 \phi_d(\gamma)} C_{44}^{s2} \left(\frac{C_{11}^s \rho^s}{E^r \rho^s} \right)^{1/2} \frac{1}{wl} \frac{d^{10}}{\eta(d)^2}. \quad (16)$$

Compared to the Q^m calculated for the first mode of the bridge, Q^d is larger by roughly a factor $(l/h)^2$. This factor is exactly what would be expected from the dipolar nature of the source. The power irradiated by an acoustic dipole where the two sources are separated by a distance $D = l/2$, as is approximately the case here, is proportional to $(D/\lambda^s)^2 = (l/2\lambda^s)^2$ times the energy irradiated by a single monopole with the same strength.²¹ Therefore, as $\lambda^s \propto l^2/h$ it results that $Q^d \propto (l/h)^2 Q^m$, as noted above. In fact, this relation between Q^d and Q^m is generally valid and because in most of the bridge and cantilever resonators found in the literature the ratio l/h is close to or larger than 10, the energy loss tends to be larger for resonators vibrating in such a way as to produce a net vertical force on the surface of the substrate as compared to a net bending moment.

C. Beyond acoustic monopoles and dipoles

The expressions for Q^m and Q^d as derived above are strictly valid for vibrational modes resulting in acoustic monopoles and dipoles, respectively. However, we can expect that Eqs. (9) and (16) provide approximate results for slightly more complex vibrations of the resonators whenever

net vertical forces or net bending moments are the prevailing disturbances acting on the surface of the substrate. This fact allows us to extend the results for some higher order vibrational modes. The estimate of Q for higher order modes is important because the use of such modes in practical devices is becoming an alternative as a means to achieve high frequency operation, specially in the UHF range.^{2,8} Focusing on the first three modes of the cantilever and bridge resonators, we can first argue that the second mode of the cantilever is going to lose energy predominantly as a monopole due to the net vertical force produced on the substrate, while the portion of the cantilever vibrating out of phase emits energy as a dipole at a much smaller rate.

In order to clarify this argument, we note that the net vertical force given by Eq. (8) is the same for every mode, the difference coming from the integral over $u_n(x)$. As noted after Eq. (9) this integral can be written as $I_{u_n} u_0 l$ were $I_{u_n} = 0.783$ for the first mode of the cantilever and equal to 0.434 for the second mode. Therefore, the net vertical force produced by the second mode is large, comparable to the force for the first mode, resulting in acoustic emissions that exceed any dipolar emissions produced by the small portion of the source close to the free end of the cantilever. In its turn, the third mode of the cantilever produces a surface force distribution that is close to the dipolar source produced by the second mode of the bridge. However, in this case, due to the lack of symmetry of this mode there results both a net vertical force and net bending moment. The vertical force is reduced compared to the lower order modes being, in this case, proportional to $I_{u_n} = 0.254$. The bending moment at the more characteristically dipolar portion of the source, limited to the left of the second node at $x = 0.868l$, is close to that found for the second mode of the bridge. As a consequence, for two limiting cases where the ratio l/h is sufficiently small (large) that the predicted energy loss due to the bending of the surface is much larger (smaller) than that due to the net vertical displacement the quality factor can be estimated using Eq. (16) [Eq. (9)]. Finally, the third mode of the bridge can be treated approximately as an acoustic tripole, a source comprised of three monopoles, two inphase and one out of phase by 180° . In this case the power emitted is that produced by a single monopole that causes a net vertical force proportional to $I_{u_n} = 0.364$.

From the analysis presented so far, some general trends on Q for higher order modes can be advanced. In general, the acoustic sources at the substrate surface are going to be n poles, corresponding to the n antinodes, each pole having approximately the same shape, and consequently intensity, along the resonator. For n odd there is a net vertical force that decreases significantly for $n \geq 3$ resulting in a very large ratio k_n/I_{u_n} and, therefore, on the increase of Q with n [see Eq. (9)]. For n even, there is no net vertical force and an increase of Q with n , proportional to $(D/\lambda^5)^{-n} \sim (l/h)^n$, is expected based on general results for the acoustic emission by multipoles.²¹

III. RESULTS AND CONCLUSIONS

In order to illustrate the relevance of the new energy loss mechanism we present in Fig. 2 contour plots for different

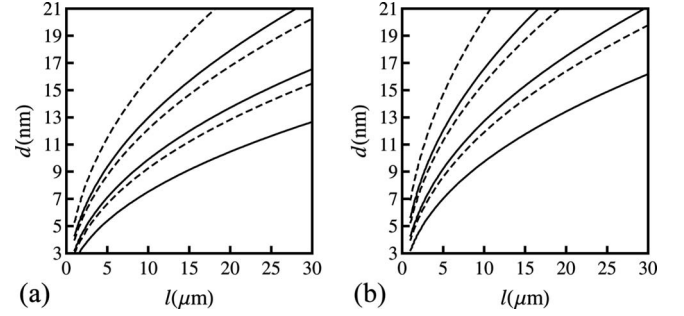


FIG. 2. Contour plot for the quality factor Q as a function of the gap d and length l of the resonator for a fixed ratio $l/w=5$, and thickness $h=0.1 \mu\text{m}$. Resonator and substrate made from (a) polysilicon and (b) gold; continuous (dashed) lines are for bridge (cantilever) resonators; the contours are for $Q=10^4$ (bottom curve), $Q=10^5$ (middle curve), and $Q=10^6$ (upper curve).

values of Q . We consider cantilever and bridge resonators made from polysilicon and gold. Polysilicon is chosen because most MEMS and NEMS are made based mostly on this material, and results based on it are representative of other forms of silicon and semiconductors such as gallium arsenide and germanium, due to their similar optical and mechanical properties. Gold is a representative of the class of soft (small Young modulus) materials that are also employed in MEMS and NEMS. Another relevant feature of gold is its high optical reflectivity, which results into a stronger Casimir force compared to a semiconductor.¹⁴ The results shown in Fig. 2 are for resonators with a constant aspect ratio $l/w=5$, which is large enough to be representative of a wide number of practical resonators,² but still sufficiently small for the point source approximation to apply. Three values of Q were chosen, encompassing values that are currently obtained for micro- and nanoresonators ($Q=10^4$ and 10^5) and those expected from technological improvements in future devices ($Q=10^6$).

What is revealed by Fig. 2 and other similar analysis we performed is that the new energy loss mechanism can be expected to be more relevant when the gaps involved are smaller than approximately 10 nm. Due to the strong dependence of Q on the gap distance, this result holds also for structures with a thickness considerably larger than the one we considered in Fig. 2 ($h=0.1 \mu\text{m}$), since a small decrease in the gap suffices to compensate for large changes in h . Because the predicted quality factor is smaller for small gaps and thin resonators, this mechanism should be more relevant for nanoresonators actuated electrostatically, since in this case nanogaps would arise naturally. In fact, as mentioned in Sec. I, electrode-to-resonator gaps as small as 20 nm were successfully fabricated for electrostatic actuation and readout of RF signals using a blade nanoresonator. It is worth to mention that this nanoresonator was very long ($l=30 \mu\text{m}$) and had a base thickness of about $1 \mu\text{m}$, demonstrating that tiny gaps can be produced for comparatively large (order of micrometer) structures, and indicating that sub-10 nm gaps can be a common feature in near future micro- and nanoresonators.

Due to the fact that the resonator mechanical energy is transferred over a vacuum gap and dissipated into a nearby

structure, this energy loss can be considered as an example of noncontact friction.²² Noncontact friction has been considered so far mainly in the context of noncontact atomic force microscopy (nc-AFM),²³ and several mechanisms involving the tip-sample interaction were considered to be the source of the energy dissipation. Acoustic energy loss was considered in this context,²² but the results derived so far are valid for small tip oscillations (harmonic approximation) and cannot be compared with, for instance, the precise experimental data presented in Ref. 24, measured using large amplitude nc-AFM. Other possible sources of noncontact friction are anelastic processes on the tip and sample, van der Waals friction resulting from fluctuating electromagnetic field,²⁵ and electrostatic friction involving electromagnetic emissions or the Joule effect. However, the bulk of experimental data cannot be consistently explained by any one of the known noncontact friction mechanisms,^{22,23,26–28} instead specific models (usually purely phenomenological models) of energy dissipation were used to explain the data for each experiment. However, some of these noncontact friction mechanisms could also contribute significantly to the total dissipation of micro- and nanoresonators.

An approximate but straightforward comparison between some of the different noncontact energy loss mechanisms can be done by comparing the friction coefficient per unit of area resulting for each mechanism. This coefficient can be obtained by modeling the resonator as an one degree of freedom system subject to a viscous damping. For the first mode of both cantilever and bridge resonators the coefficient of friction due to the acoustic losses is given by $\gamma = m_{eff}\omega_1/(QS)$, where $m_{eff} = cphwl$ denotes the effective mass, with $c=0.396$ for bridge and $c=0.250$ for cantilever, Q corresponds to the quality factor and $S=wl$ to the area. The resulting γ is proportional to the area, and for a microresonator made from gold with $l=5w=5 \mu\text{m}$ suspended 10 nm above a gold substrate it results to be $\gamma=0.32 \text{ kg s}^{-1} \text{ m}^{-2}$. For comparison, the corresponding friction coefficient due to

the van der Waals friction assuming clean gold surfaces is approximately $\gamma^{vdW}=10^{-5} \text{ kg s}^{-1} \text{ m}^{-2}$ at a temperature $T=300 \text{ K}$.²² For semiconductors γ^{vdW} increases, and for silicon carbide it is predicted to be one order of magnitude larger than for good conductors. Almost exactly the opposite of that is observed for γ which is approximately one order of magnitude smaller for a semiconductor like silicon as compared to gold. It is worth to mention that the van der Waals friction is expected to increase by orders of magnitude under certain circumstances,²² for instance, with surface contamination, therefore giving rise to a significant energy loss channel, possibly comparing to or surpassing the energy loss mechanism analyzed in this work. It is also interesting to note that the Joule dissipation,²⁹ due to the Joule effect, investigated in the context of nc-AFM, has already been incorporated into the modeling of practical micro- and nanoresonators actuated electrostatically. In this last case the time-varying electric field, due to resonator vibration, results into a time-varying charge at the electrodes and, consequently, an electric current. The vibrational energy is dissipated by the Joule effect as this current flows through the structure facing the electric resistance R forming the equivalent RLC circuit.³⁰

We conclude by noting that the energy loss mechanism we investigated can be relevant for a wide class of future NEMS and MEMS where moving parts are separated by distances at the nanoscale. The ubiquitous Casimir force can produce the coupling between the moving parts and nearby structures through which mechanical energy can be lost in ways that were not addressed in this work. Therefore, further investigations on the implications of this energy loss mechanism on different systems should be performed.

ACKNOWLEDGMENT

The author acknowledges the financial support by the Conselho Nacional de Desenvolvimento Científico e Tecnológico, CNPq-Brazil.

*andre.gusso@pq.cnpq.br

¹H. G. Craighead, *Science* **290**, 1532 (2000).

²C. T.-C. Nguyen, *IEEE Trans. Ultrason. Ferroelectr. Freq. Control* **54**, 251 (2007); A.-C. Wong and Clark T.-C. Nguyen, *J. Microelectromech. Syst.* **13**, 100 (2004); F. D. Bannon, J. R. Clark, and C. T.-C. Nguyen, *IEEE J. Solid-state Circuits* **35**, 512 (2000).

³X. L. Feng, R. He, P. Yang, and M. L. Roukes, *Nano Lett.* **7**, 1953 (2007).

⁴S. S. Verbridge, D. F. Shapiro, H. G. Craighead, and J. M. Parpia, *Nano Lett.* **7**, 1728 (2007).

⁵S. M. Tanner, J. M. Gray, C. T. Rogers, K. A. Bertness, and N. A. Sanford, *Appl. Phys. Lett.* **91**, 203117 (2007).

⁶P. Mohanty, D. A. Harrington, K. L. Ekinci, Y. T. Yang, M. J. Murphy, and M. L. Roukes, *Phys. Rev. B* **66**, 085416 (2002).

⁷V. Agache, B. Legrand, D. Collard, L. Buchaillet, and H. Fujita, *Appl. Phys. Lett.* **86**, 213104 (2005).

⁸S. Y. No and F. Ayazi, in *Proceedings of the 2001 1st IEEE*

Conference on Nanotechnology, Maui, Hawaii, 2001 (IEEE, Piscataway, NJ, 2001), p. 489.

⁹A. I. Volokitin, B. N. J. Persson, and H. Ueba, *Phys. Rev. B* **73**, 165423 (2006).

¹⁰M. Bordag, U. Mohideen, and V. M. Mostepanenko, *Phys. Rep.* **353**, 1 (2001).

¹¹A. Gusso and G. J. Delben, *Sens. Actuators, A* **135**, 792 (2007).

¹²R. C. Batra, M. Porfiri, and D. Spinello, *Smart Mater. Struct.* **16**, R23 (2007).

¹³E. M. Lifshitz, *Sov. Phys. JETP* **2**, 73 (1956).

¹⁴A. Gusso and G. J. Delben, *J. Phys. D* **41**, 175405 (2008).

¹⁵K. F. Graff, *Wave Motion in Elastic Solids* (Dover, New York, 1991).

¹⁶G. F. Miller and H. Pursey, *Proc. R. Soc. London, Ser. A* **223**, 521 (1954); **233**, 55 (1955).

¹⁷J. A. Judge, D. M. Photiadis, J. F. Vignola, B. H. Houston, and J. Jarzynski, *J. Appl. Phys.* **101**, 013521 (2007).

¹⁸Z. Hao and Y. Xu, *J. Sound Vib.* **322**, 196 (2009).

- ¹⁹S. C. Hunter, *J. Mech. Phys. Solids* **5**, 162 (1957).
- ²⁰G. N. Bycroft, *Philos. Trans. R. Soc. London, Ser. A* **248**, 327 (1956).
- ²¹F. Fahy, *Foundations of Engineering Acoustics* (Elsevier, London, 2001).
- ²²A. I. Volokitin and B. N. J. Persson, *Rev. Mod. Phys.* **79**, 1291 (2007).
- ²³*Springer Handbook of Nanotechnology*, edited by B. Bhushan (Springer-Verlag, Heidelberg, 2004).
- ²⁴B. Gotsmann and H. Fuchs, *Phys. Rev. Lett.* **86**, 2597 (2001).
- ²⁵The van der Waals friction should not be confused with the acoustic energy loss mediated by Casimir/van der Waals force we investigate in this work. The van der Waals friction has a physical origin similar to that of Casimir/van der Waals force, the fluctuations of the electromagnetic field. However, van der Waals friction is mostly determined by the exchange of Doppler-shifted real photons due to the relative motion of the bodies (Ref. 22).
- ²⁶P. M. Hoffmann, S. Jeffery, J. B. Pethica, H. Özgür Özer, and A. Oral, *Phys. Rev. Lett.* **87**, 265502 (2001).
- ²⁷O. Pfeiffer, L. Nony, R. Bennewitz, A. Baratoff, and E. Meyer, *Nanotechnology* **15**, S101 (2004).
- ²⁸R. Garcia, C. J. Gómez, N. F. Martinez, S. Patil, C. Dietz, and R. Magerle, *Phys. Rev. Lett.* **97**, 016103 (2006).
- ²⁹W. Denk and D. W. Pohl, *Appl. Phys. Lett.* **59**, 2171 (1991).
- ³⁰H. J. De Los Santos, *Introduction to Microelectromechanical Microwave Systems* (Artec House, Norwood, 2004).